Enhanced velocity based pore pressure prediction using lithofacies clustering: A case study from a reservoir with complex lithology in Dezful Embayment, SW Iran

Farid ArabAmeri[a], Hamid Soleymani[b,*], Behzad Tokhmechi[c]

[a] *University of Tehran, Iran*
[b] *The Graduate Center, City University of New York, U.S.A*
[c] *Faculty of Mining, Petroleum and Geophysics Engineering, Shahrood University of Technology, Iran*

Abstract

Velocity based pore pressure prediction methods are widely accepted as a routine technique in the petroleum industry. Despite recent improvements, still, literature suffer from inconsistencies and uncertainties mostly arise from velocity anomalies due to complex lithostratigraphic setting or presence of various formation fluids. The primary goal of this paper is to improve the accuracy and reliability of the conventional Bowers and Tau methods in a reservoir with complex lithology. Our proposed workflow aims to improve the accuracy of the estimations by clustering the input data based on specific petrophysical characteristics. We show since each major zones at the offset test wells have a distinct *compaction trend*, empirical constants in Bowers and Tau methods can be calibrated for each cluster rather than the whole stratigraphic column. The clustering task was done by statistical analyses of a suite of well logs and validated with core derived lithologies. To find the best clustering algorithm, we applied and compared five techniques namely, K-means, basic sequential algorithmic scheme, single, and complete linkage hierarchical. We found that the self-organizing map (SOM) method provides the best results by maximizing lithology likelihood within each cluster and improve the overall accuracy of the Bowers and Tau methods. This research also aims to provide a systematic comparison of the mentioned clustering algorithms based on their ability in distinguishing various lithofacies. We also try to minimize the user interference in the process of clustering multiple lithofacies and improve the reproducibility of the results and demonstrate the capability of the proposed method through a case study in a reservoir in the Southwest of Iran. Satisfactory results of this study offer a safe ground for implementation of the proposed method in other sedimentary basins.

Keywords: Pore Pressure, Bowers Method, Tau Method, Self-Organizing Map, Lithofacies

*Corresponding author
Email addresses: farid.ameri@alumni.ut.ac.ir (Farid ArabAmeri), hsolyemani@gradcenter.cuny.edu (Hamid Soleymani), tokhmechi@ut.ac.ir (Behzad Tokhmechi)

1. Introduction

Pore pressure prediction is an active and longstanding research area in the Earth science, and it has been the focus of the petroleum industry since the early days of exploration and exploitation. Blowouts, kicks, borehole washouts, wellbore breakout and stuck pipe (Oughton et al., 2015) are just some issues that may occur while encountering unexpected fluid pressure anomalies during drilling. To reduce the associated risks of drilling a robust mud plan and casing design is required as a part of every drilling operation (Nguyen et al., 2015; Wild et al., 2015). Today a reliable estimate of pore pressure before drilling is not just a routine to increase safety and cost efficiency of the operation, but it also provides an unparalleled source of information in the exploration phase. Pore pressure data can be used to inform suitable production method, maximum hydrocarbon column in the reservoir, integrity and sealing capacity of the caprock, and its economic threshold (Holm, 1998; Hao et al., 2015; Guglielmi et al., 2015; Cranganu and Soleymani, 2015; Cranganu et al., 2014).

One of the remarkable early contributions in the estimation of pore pressure was made by Hottmann et al. (1965). They documented that the porosity decrease as a function of depth in sediments from the southern Louisiana gulf coast and by extension, applied their observations to other sedimentary basins. They further state that any deviations from the normal trend could be associated with abnormal pore pressure. Eaton et al. (1972) showed the application of deep resistivity log data in shale sediments of the Gulf of Mexico as an indicator of higher pore pressure. They also introduced an empirical equation to derive pore pressure by demonstrating the relationship between effective stress and sonic-transit-time. Bowers et al. (1995) proposed a power-law relationship between compressional velocity and effective stress by calculating the overburden stress and predict the pore pressure at offset well locations. Similarly, Giles et al. (1998) introduced a compound mudline and matrix-transit-time variable (Tau) as a first-order effective stress versus velocity power-law relationship. Later, Boitnott et al. (2009) improved Bowers method by considering a normal compaction trend that is asymptotic to matrix velocities and can provide a better representation of the physical properties of the rocks.

Various authors reported a successful application of integrated velocity data by incorporating various available velocity sources (e.g., sonic logs, seismic velocity) to estimate pore pressure (Riahi and Soleymani, 2011; Soleymani and Riahi, 2012; Liu et al., 2018). However, generating a comprehensive velocity model compound of various type of data is not straightforward. For instance, One should keep in mind that above methods heavily depend on the relationship between porosity and pore pressure (Mannon and Young, 2017; Wang and Wang, 2015; Zhao et al., 2014) which may not be a valid assumption in case of complex lithology (Obradors-Prats et al., 2016). Also, the presence of secondary phases (e.g., methane, brine) introduce a major uncertainty and may lead to false interpretation of the velocity data and inaccurate pore pressure estimation (Nour and AlBinHassan, 2013). Accurate calibration of Bowers or Tau relationships for a specific geological setting is an essential step in velocity based pore pressure estimation (Sheng et al., 2017), and it can reduce the associated uncertainties significantly.

Application of the unsupervised lithofacies classification using statistical methods have

shown before (Aminzadeh and De Groot, 2006; Dell'Aversana et al., 2018; Bohling and Dubois, 2003; Cranganu, 2013); however, no previous study has investigated the results of lithofacies classification in estimating pore pressure. In this study, we aim to tackle shortcomings of the conventional methods by lithological classification of the reservoir rocks and to generate empirical constant of velocity versus effective stress relationship for every major cluster. Our workflow (figure 1) is comprised of following steps: (1) acquiring, editing, and processing sonic logs and seismic velocity data; (2) calculating overburden stress, and effective stress at well locations; (3) clustering well logs that reflect lithology and fluid content, namely compressional velocity, gamma ray, laterolog deep, neutron porosity; (4) determining the number of nodes and iterations as well as the optimum number of clusters by comparing the results with core derived lithologies; (5) calibrating empirical constants of Bowers and Tau methods by applying a power regression model on velocity versus effective stress scatter plot for each cluster; (6) using the acquired relationships to predict effective stress with respect to each cluster; (7) calculating pore pressure by subtracting the calculated overburden stress from effective stress.

We present the application of the proposed method as a case study in a reservoir with diverse lithology, fluid content, and saturation and show that the method can improve the prediction results. We also provide a comparison between five popular clustering algorithms, namely K-means, basic sequential algorithmic scheme, single, and complete linkage hierarchical based on their performance in distinguishing various lithofacies.

2. Material and methods

A general geological description of the studied field is provided in along with the discussion on stratigraphy and lithology. We also detailed various available data (e.g., well logs, well tests, seismic, and core data) and calculations necessary to predict pore pressure. The theory of Bowers and Tau methods are presented along with a discussion on accuracy of the predictions in Asmari reservoir. To further describe the method and to carryout the calculations we discuss the principles of the above mentioned clustering methods and apply them on our well data. To choose the best clustering method, we compared the resultant clusters with core derived lithologies. Finally, we use the clusters calculated by the best method to calibrate empirical constants of Bowers and Tau methods.

2.1. Geological settings

Mansouri oil field is located in the south of Ahwaz in Dezful embayment in Iran with the production rate of over 110,000 bbl/day. It follows the northwest-southeast trend of Zagros, with the length of 30 km and width of 5 km. It consists of two major reservoirs namely Asmari and Bangestan (Ahmadi et al., 2012). Investigating lateral lithology variations, complex stratigraphy, and pore pressure of the Asmari formation throughout the basin is the main focus of this study and a major challenge for drilling companies. Location of the Mansouri oilfield on the map and position of the wells used in this study have shown on top of the Asmari formation (figure 2).

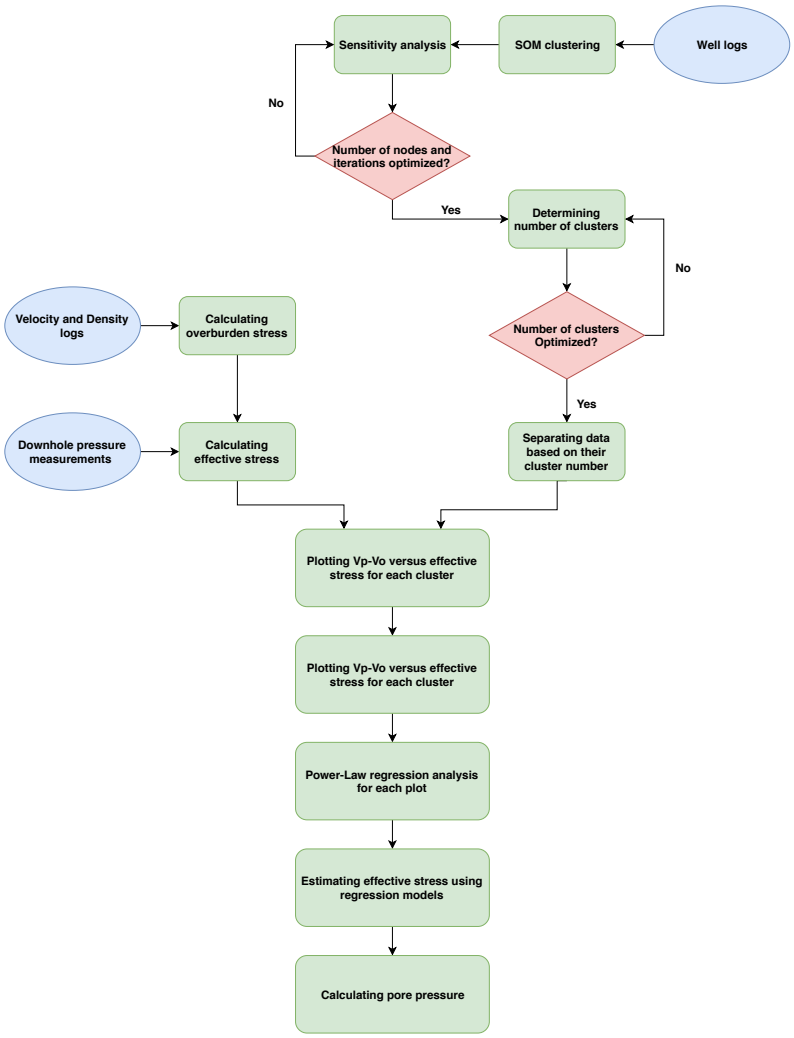

Figure 1: Our proposed workflow for pore pressure prediction in formations with complex lithostratigraphy.

Asmari is an asymmetric anticline dipping around 0-10 deg at both ends (Ahmadi et al., 2012). A comprehensive study by Van Buchem et al. (2010) indicated that the Oligocene-Miocene Asmari formation mostly consists of shallow-water carbonate depositions and siliciclastic. While sandstones are deposited on top of the carbonate platform as lobes or bars along margins of the intrashelf basin or as turbidites in the basin center, the carbonates are mostly formed in the platform margin and can be massive and grainy and form prograding clinoforms.

The Asamri reservoir has a complex stratigraphic architecture, which consists of three Oligocene and three Miocene sequences. Gacio-eustatic sea level fluctuations govern the stratigraphic architecture of these sequences and allot the distribution of the different lithologies (Van Buchem et al., 2010). These different rock types were formed in low- to high-energy homoclinal ramp environments (Kangazian and Pasandideh, 2016). Major depositional en-

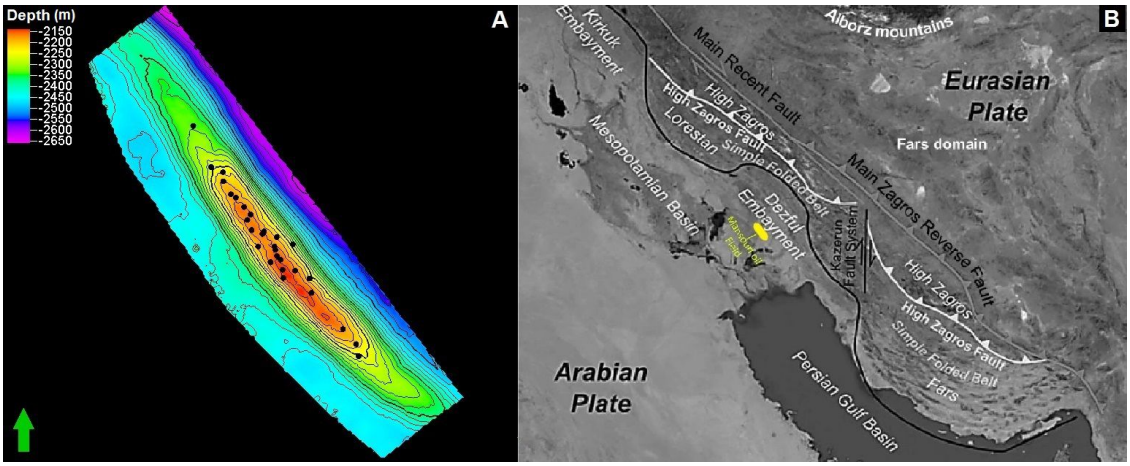

Figure 2: Schematic map, well locations (black dots), and top of the reservoir. (A) Top of the Asmari reservoir picked from the well data and 3-D seismic. (B) Approximate location of the Mansouri oil field (Saberhosseini et al., 2013).

vironments include tidal-flat, lagoonal shoal, semi-restricted, and open-marine was formed along the foreland basin during the collision of Arabian plate and Iranian micro-continent (figure 3). It appears lithological heterogeneity, complex geometries, early and late diagenetic alterations have cause Asmari formation to be considered a complex formation (Van Buchem et al., 2010). These changes reflect the progradation dynamics of the platform in the reservoir (Ehrenberg et al., 2007).

Overall the reservoir can be divided into eight zones and sixteen subzones based on age and microfossils studies. Figure 4 show the scatter plot of V_p versus density at a well location and major zones of the reservoir. Petrographic analysis of core samples and lithofacies studies confirm the periodic occurrence of limestone, dolomite, sandstone, and shale. The first member mostly consists of carbonates, second, third, fourth, and the fifth mostly consist of sandstones, the sixth member mostly consists of limestone, dolomite, and shale, the seventh member consists of limestone, sandstone, and shale, whereas, the eighth member consists of limestone and shale. While Anhydrite is mostly present in pore spaces of the fifth member, they could also be observed in some sandstone and carbonate members. Consolidation of sandstones in member two and three is generally better in the west side of the reservoir than its east side. Shale interlayers are also present in sandstone members, especially in top and bottom of the member three.

2.2. Dataset

The available dataset is consist of post-stack 3D seismic with 2041 in-lines and 552 cross-lines with the spatial resolution of 25 m in in-line and cross-line directions and temporal resolution of 4 m sec. We also had access to processing information including stacking velocities, interpretation of major reflectors, seismic wavelet and acoustic impedance inversion. Well data was consist of complete suite of well logs including density, electrode resistivity devices (LLD, LLS, MSFL), gamma ray, neutron porosity, compressional velocity, photoelec-

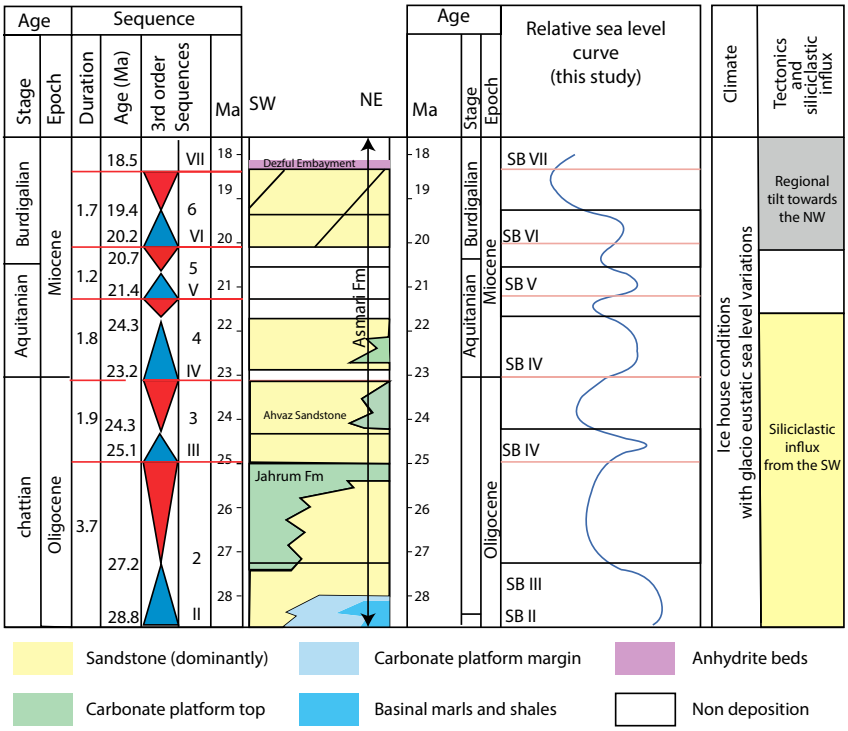

Figure 3: Chronostratigraphic scheme, sequence stratigraphy and sea level variation of Asmari formation in Dezful embayment. These sediments were deposited during ice-house conditions. The cyclic occurrence of mixed lithologies and sequences is common during ice-house conditions (J.Doyle and H.Roberts, 1988). Seven stratigraphy sequences were found in the studied area correspond to tract cycles and separated by six sequence boundaries. Sea level fluctuations have a substantial effect on the vertical lithology variation of the Asmari formation. As the sea level falls, terrigenous sediments are deposited on shelves and basins. In contrast, with sea levels rise, carbonates are deposited (Tucker, 2003). It has been suggested that high amplitude sea level fluctuations in relatively short periods of time are the main reason behind the complex lithostratigraphy of the Asmari formation (figure modified from Van Buchem et al., 2010).

tric absorption factor (PEF data was not available for all wells), and caliper measurements (a total number of 28 wells were analysed). Downhole measurements including repetitive formation test (RFT), core measurements including special core analysis (SCAL), and X-ray powder diffraction (XRD) were available at five well locations.

2.3. Conventional Bowers and Tau methods

Bowers et al. (1995) showed a drop in sonic velocity without decreasing the bulk density might be an indicator of unloading, and this phenomenon might be a direct result of fluid expansion. They also derived the effective stress from measured pore pressure data and calculated overburden stress (equation 3) based on sonic interval velocities from well log data in the Gulf of Mexico (equation 2). They further demonstrated that the sonic velocity and effective stress have the following power-law relationship:

$$V_p = V_0 + A\sigma_{eff}^{B} \qquad 1$$

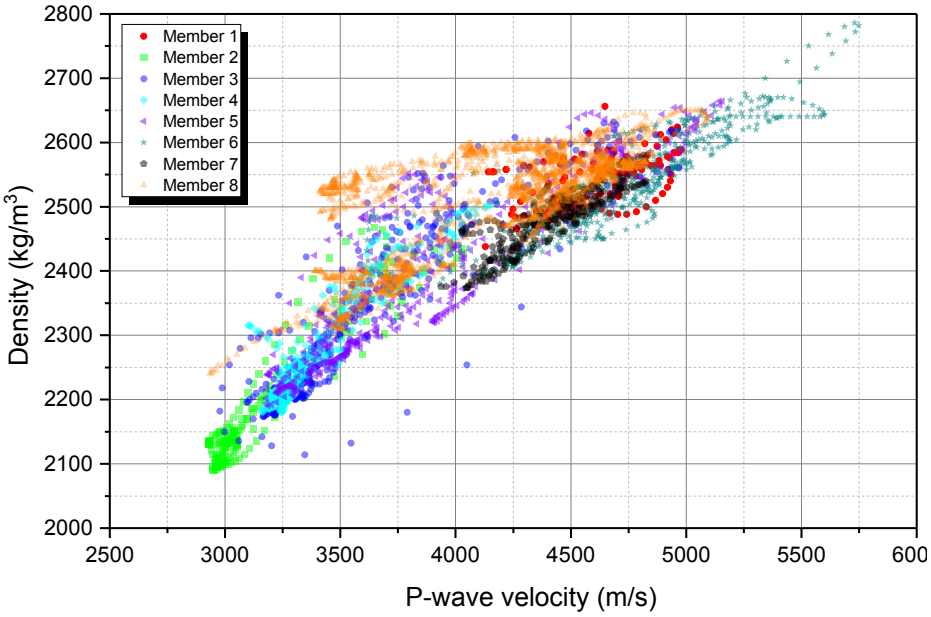

Figure 4: Scatter plot of V_p versus density at a well location. Relatively distinct spread of some members suggests the presence of various lithological units within the data. Note that zones are classified based on age and microfossils studies.

where V_p is compressional velocity at a given depth, V_0 is compressional velocity in mudline or unconsolidated saturated surface sediments, σ_e is effective stress, A $(m^2.s/kg)$ and B (dimensionless) are empirical constants calibrated with offset velocity versus effective stress data (Chopra and Huffman, 2006).

Considering equation 1, effective stress can be calculated using compressional velocity. The calculated effective stress can be used to find pore pressure using the equation below (Terzaghi, 1925):

$$\sigma_e = \sigma_o - \alpha P_p \tag{2}$$

where α is Biot's constant and according to (Bowers, 1995) α equals one in the reservoir conditions, P_p is pore pressure, σ_o is overburden stress and can be calculated using equation 3:

$$\sigma_o = \int_0^z \rho g dz \tag{3}$$

where ρ is density, g is gravitational acceleration and z is depth.

The conventional workflow starts with editing the acquired data by careful investigation of caliper log to locate the wellbore collapses, and identify outlier data points outside the three standard deviations from the mean (Wang and Wang, 2015). Then, we calibrate the Bowers relationship (equation 1) in offset wells via regression analysis of the calculated effective stress at depths with available P-wave velocity (figure 5A). The results of the regression analysis of velocity versus effective stress confirm that the Bowers calibration is not statistically

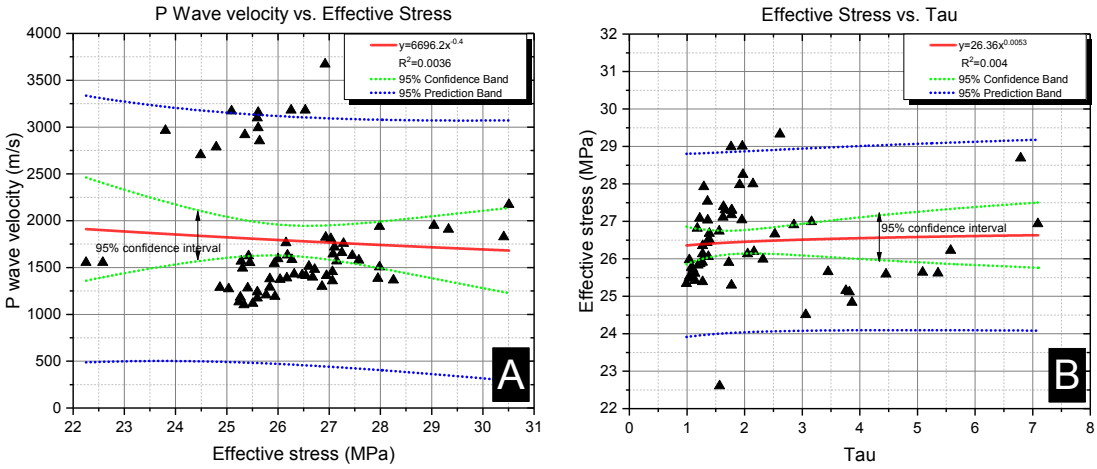

Figure 5: Velocity versus effective stress for available well data. Bowers (A) and Tau (B) methods does not provide a suitable fit, and the regression is not statistically representative of the data.

significant. Thus, calculating pore pressure based on the derived relationship results in introducing a major uncertainty.

Alternatively, we applied Tau method (equation 4) on the same dataset. Giles et al. (1998) introduced new parameter τ, and coupled the velocity to effective stress via empirical constants as:

$$\sigma_e = A\tau^B \tag{4}$$

where A and B are empirical constants and τ can be calculated from equation 5:

$$\tau = \frac{C - \Delta t}{\Delta t - D} \tag{5}$$

where Δt is the compressional transit time, acquired from a sonic well log or seismic velocities, C is the constant related to the mud-line transit time and D is constant related to matrix transit time. To apply this method, it is necessary to calculate the matrix and mud-line transit times and obtain empirical constants (A and B). Mud-line transit time can also express as the transit time in saturated unconsolidated sediments in the surface (Zhang, 2011; Ugwu, 2015). Cross-plot of the Tau versus effective stress figure 5B show that the regression results are also statistically insignificant.

2.4. Clustering methods

We hypothesized statistically insignificant regression results are associated with sharp lithology transitions in relatively short intervals. Lithology can cause variations in P-wave velocity, leading to major uncertainty in conventional pore pressure prediction methods. This assumption is also in agreement with core derived lithologies. Hence, to reduce the uncertainties associated with the effect of transient lithology on velocity, we derived various major lithological units in the reservoir column using multiple statistical clustering methods,

then, we applied the Tau, and Bowers methods on derived units individually. Multi-variable clustering methods provide a comprehensive basis to classify a multi-dimensional dataset (e.g., well logs, core data, seismic). Five clustering methods namely, complete linkage hierarchical, single linkage hierarchical, K-means, basic sequential algorithmic scheme, and SOM were applied on well logs (i.e., density, gamma ray, neutron porosity and sonic) and the accuracy of recognizing different lithologies was analyzed by comparing the results with data obtained from cores.

2.4.1. Self-organizing maps

The SOM clustering is a well-known unsupervised learning method from the family of artificial neural networks (Kohonen, 1998). Various workers document the geophysical application of the SOM. As an early adopter Coléou et al. (2003) used it as a tool in seismic interpretation and called it " an essential tool for unsupervised seismic analysis." Similarly, other scholars benefit from SOM method in the seismic-facies analysis (Saraswat and Sen, 2012) and recognition of seismic patterns (Kourki and Riahi, 2014; Yang et al., 1991). Jouini and Keskes (2017) utilized the SOM in characterizing the mechanical properties of the reservoir rocks. Sfidari et al. (2014) demonstrated that SOM could provide much better results for lithofacies clustering than other clustering methods.

SOM consist of a network of neurons connected with a rectangular or hexagonal connection. In the first iteration, weights are either allocated to neurons randomly or through the generated principal component eigenvectors of the subspace. Then, the Euclidean distance between the provided input and the weight vectors are measured, and the nearest neuron will be selected. The selected neuron and other neurons in its neighborhood alter to become as similar as the input vector. Through multiple iterations, the weights of the neurons converge as the neighborhood of the best matching unit (BMU) shrinks (Ciampi and Lechevallier, 2000). The robustness of SOM clustering method could be associated with its characterized non-linear projection from the higher dimensional space of inputs to a low dimensional grid, which facilitates the discovery of hidden patterns in the input data (Kohonen and Honkela, 2007; Moghimidarzi et al., 2016). The SOM proved to be able to handle large datasets with outliers effectively (Shahreza et al., 2011; Oyana et al., 2012), and it has been applied successfully in complex structures (Tasdemir and Merényi, 2009).

To implement the SOM clustering algorithm and calibrate the constants of Bowers and Tau methods, we ran the clustering analysis on all of the available wells. The SOM algorithm was trained with weight and bias learning rules, and the mean-squared-error calculated as a metric to measure the goodness of training. Sensitivity analysis was also carried out to determine the optimum number of nodes and iterations (figure 6). Figure 6A shows the quantization error decreases remarkably with increasing number of nodes. Similarly, the topological error decreases slightly and stabilize by increasing the number of nodes. Figure 6B demonstrates the changes in topological and quantization error as a function of iteration. Figure 6 also shows the quantization error decreases significantly with the number of iteration (especially within the first 400 iterations) while topological error decreases marginally. To validate the results, core samples with XRD measurements were selected, and compared with the correspondent lithologies derived from a cluster at the same depth. The selected clusters

and their respective lithology information were used to validate other clusters in available wells. Table 1 summarizes the dominant lithology in each cluster.

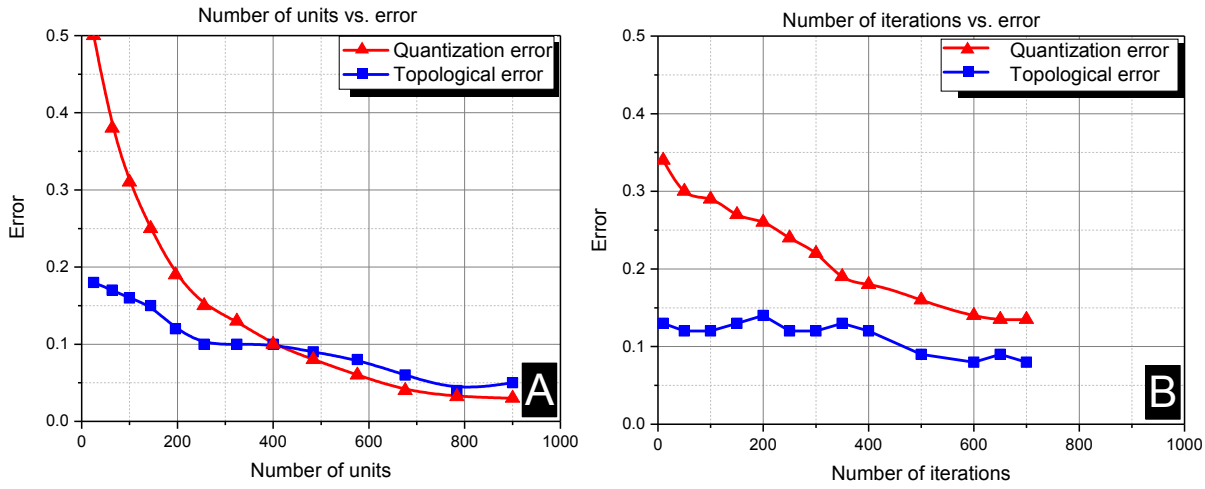

Figure 6: Quantization error and topological error variation versus the number of units (A) and a number of iterations (B).

Cluster #	Lithology type
1	Shale
2	Dolomite and Limestone
3	Shale and Shaly Limestone
4	Sandstone
5	Shaly Sandstone

Table 1: SOM clusters and their respective lithologies.

2.4.2. Modified basic sequential algorithmic scheme

In the modified basic sequential algorithmic scheme (M-BSAS), each cluster is represented by mean of the assigned vector (Ahmadi and Berangi, 2008). The algorithm calculates the distance between each data point and the cluster centroid. While the maximum number of clusters has not been reached and the distance was larger than a pre-defined threshold of dissimilarity, a new cluster will be formed, and the data point will be assigned to the nearest cluster (Theodoridis et al., 2010). Note that the method is heavily dependent on the order of presenting data and user-defined threshold. The algorithm consists of two phases; (1) part of the data are used to determine the maximum number of clusters. (2) The unassigned data are allocated to their appropriate clusters (appendix) (Kainulainen and Kainulainen, 2002). Sarparandeh and Hezarkhani (2016) implemented this method for delineating lithology and exploring rare elements. Jin (1994) also implemented BSAS for two-dimensional subsidence

analysis. This method was implemented in Matlab software. The input data consisted of five well logs including P-wave transit time, laterolog deep, neutron porosity, density, and gamma-ray.

2.4.3. K-means

This algorithm uses k pre-defined number of clusters from a set of n, d-dimensional data points with the objective of minimizing the Euclidean distance between cluster centers and data points (Hong et al., 2017). The underlying algorithm works by allocating each data point to the nearest cluster, then introduces new centers for each cluster (appendix). These iterations continue until centroids no longer change (Reddy et al., 2012). Di Giuseppe et al. (2014), successfully utilized k-means algorithm to distinguish geological structures with different rheologies. Wohlberg et al. (2006) were also showed that k-means is a robust tool for delineating geological features. This method was applied to the same dataset as M-BSAS using Matlab software.

2.4.4. Single linkage and complete linkage hierarchical methods

Single linkage and complete linkage hierarchical methods belong to a distinct type of hierarchical clustering called agglomerative. In this clustering method, each data point is considered as a cluster (Fouedjio, 2016). In each iteration, the distance between the two clusters is calculated, and the two clusters with the nearest distance merge. This process continues until the pre-defined number of clusters are obtained (Carlsson et al., 2017). A notable technique in this family is the complete linkage method which is different from the single linkage in calculating the distance. While in single linkage method the two clusters with the closest members have the smallest distance (appendix), in complete linkage method, the largest dissimilarity between two identical features of two data points is calculated (appendix) (Fouedjio, 2016). This method were applied on the same dataset as M-BSAS using Matlab software. The dendrogram of the single linkage hierarchical method and the cut-off value shown in figure 7.

2.5. Comparing clustering methods

We used two criteria to compare the clustering methods: (1) their ability to recognize independent velocity versus effective stress trends (i.e., R-squared of the regression trend), (2) delineating lithologies verified by core data. By analyzing the similarity of the lithology within clusters, error for each method was calculated, and the optimum number of clusters was determined (table 2). Analysis of various clustering methods indicates that SOM provides better results in terms of delineating various lithologies compared to other previously mentioned techniques.

2.6. Enhanced pore pressure prediction

To calculate pore pressure with respect to newly established clusters, velocity versus effective stress scatter plots were created for each cluster independently. However, due to lack of RFT data in cluster three and five, power regression fit was applied only to cluster one, two and four. Thus, to obtain a continuous prediction model within the reservoir,

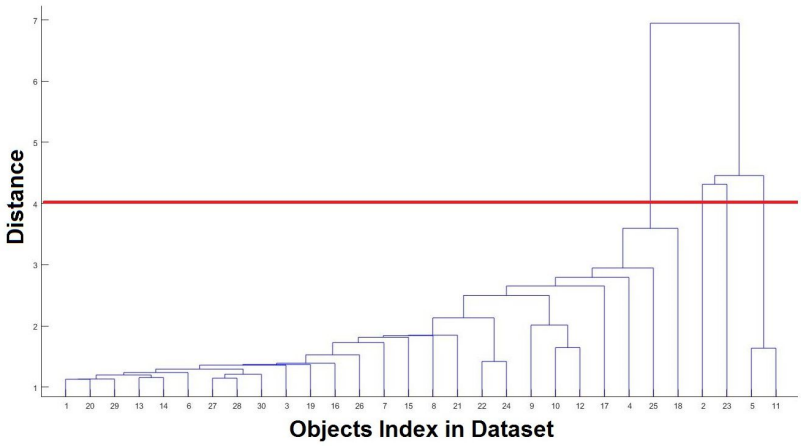

Figure 7: Dendrogram of single linkage hierarchical method. The horizontal axis represents the indices of the objects in the original data set, and the vertical axis represents the distance between the objects. Cut off line is shown with red color, indicates the selected number of clusters.

Bowers equation for cluster three and five was obtained from other clusters with similar lithology. Velocity versus effective stress trends and similarity analysis of the well logs in different clusters show that the cluster five is relatively similar to cluster two, and cluster three is relatively similar to cluster four. Figure 9 demonstrates regression results for cluster one, two and four.

After finding the empirical constants in equation 1 for each cluster, we calculated effective stress for each data point in our test wells based on cluster number, their respective equation, and obtained pore pressure from equation 2. Figure 11A demonstrates the final pore pressure estimation (red curve) for all clusters in the test well along with RFT measurements.

To calculate pore pressure using Tau method, we carried out regression analysis to find empirical constants of equation 4 for each cluster. Figure 10A, B, and C show results for clusters one, two and four respectively. At this point, pore pressure can be calculated by following the procedure described in the previous section. Estimated pore pressure using modified Tau method at the test well is shown in figure 11B.

3. Discussion and results

Lithology, porosity, and fluid content variations have a significant effect on the accuracy and precision of pore pressure estimation based on P-wave velocity (Obradors-Prats et al., 2016; Wang and Wang, 2015; Oloruntobi et al., 2018). This can be explained by the strong dependence of P-wave velocity with lithological and geomechanical parameters. Therefore, interpretation of any derived parameters from velocity data requires a detailed understanding of the stratigraphy, lithology, and geomechanical history of the prospect. In the studied reservoir, the interplay of diverse lithostratigraphic units is considered to be a major complication in using conventional protocols. To tackle this problem we implement several clustering methods namely, complete linkage hierarchical, single linkage hierarchical,

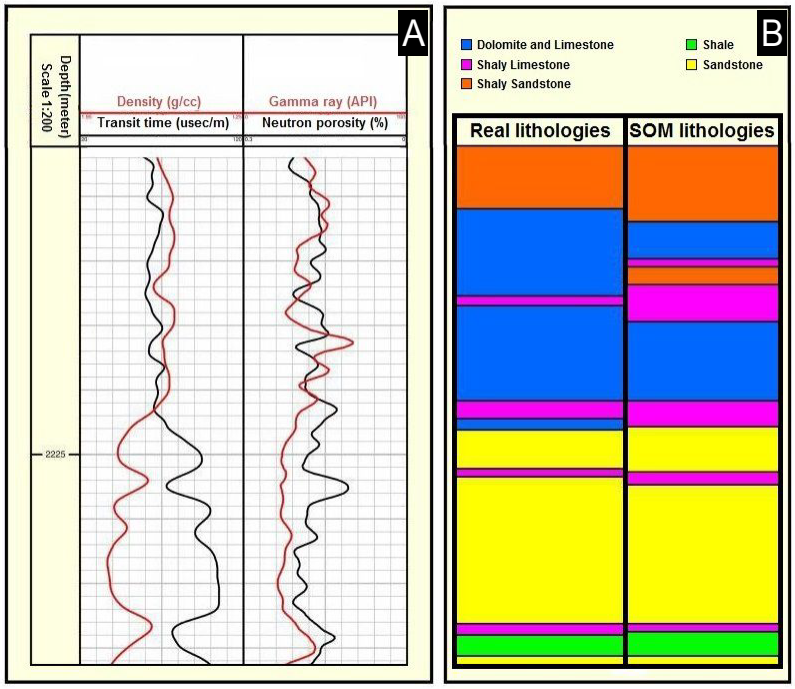

Figure 8: Comparison between well logs, SOM clusters, and core derived lithologies. (A) Transient time and neutron porosity versus depth at a selected well. (B) Real lithologies derived core data and SOM clustering results.

K-means, basic sequential algorithmic scheme, and SOM on five well logs, and their results were compared based on the capacity to distinguish various P-wave velocity versus effective stress trends. These trends then juxtaposed into clusters with similar lithological characteristics. The error between the core derived lithologies, and the dominant lithology of the clusters was evaluated to determine the optimum number of clusters and the best clustering method. The summary of the overall performance of different clustering algorithms and their optimum number of clusters is provided in table 2.

Algorithm	Performance ranking	Optimum clusters
SOM	1	5
K-means	2	7
M-BSAS	3	6
complete linkage hierarchical	4	3
single linkage hierarchical	5	4

Table 2: Performance ranking for different clustering methods based on their capability to delineate lithological units and their respective optimum number of clusters.

Our findings show that the self-organizing map (SOM) provides the best results by maximizing lithology likelihood within each cluster and improves the efficiency of the Bowers

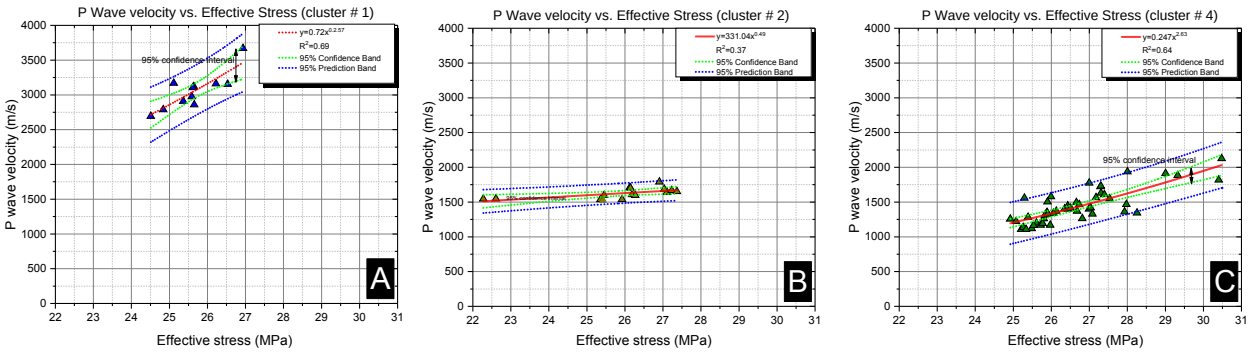

Figure 9: Regression analysis for $V_p - V_0 (V_0 \approx 1720\,\mathrm{m\,s^{-1}})$ versus effective stress for cluster one (A), two (B), and four (C).

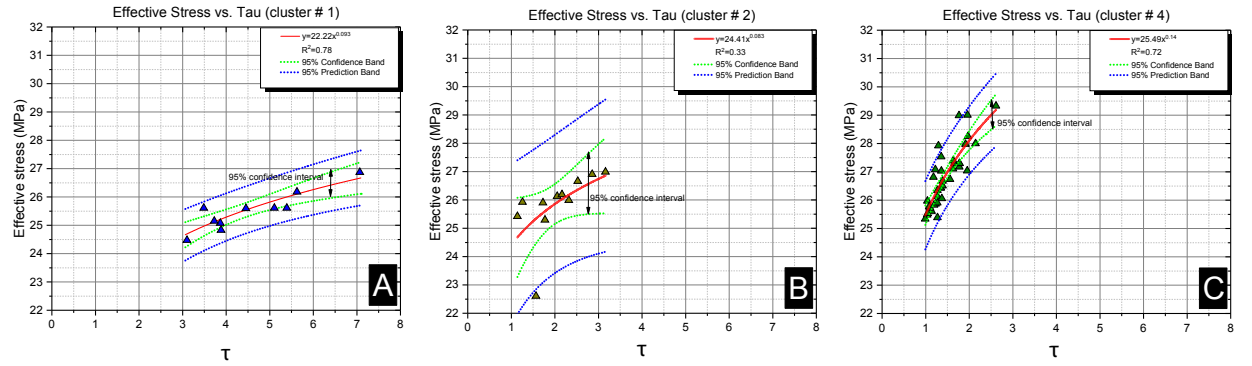

Figure 10: Regression analysis effective stress versus Tau for cluster one (A), two (B), and four (C).

and Tau methods. A notable advantage of this method is preserving the topology of high dimensional space by mapping the initial data set into a two-dimensional space with the rectangular or hexagonal structure of weighted neurons (Kohonen and Somervuo, 2002).

In this study, we successfully applied SOM algorithm and concluded that the method could handle structural complexities while showing less sensitivity to unwanted data. This observation is in accord with findings of Abu Abbas (2008).

To analysis the clustering results, we associate each cluster with a specific lithology; however, interpretation of well logs suggest each unit comprised of the specific lithology along with the small percentage of secondary units. We interpret these units as a thin layer within the major members (section 2.1). We also observed relatively high velocities in cluster one along with high electrical resistivity and low porosity (figure 12). Base on these observations we interpret these shale units as being highly siliceous with low clay content (less than 45% based on a gamma-ray log) (Nelson, 2010).

The robustness of Bowers and Tau calibration regressions (R-squared) in the modified method (figure 9 and 10) suggest a significant improvement in cluster one (mostly shale) and

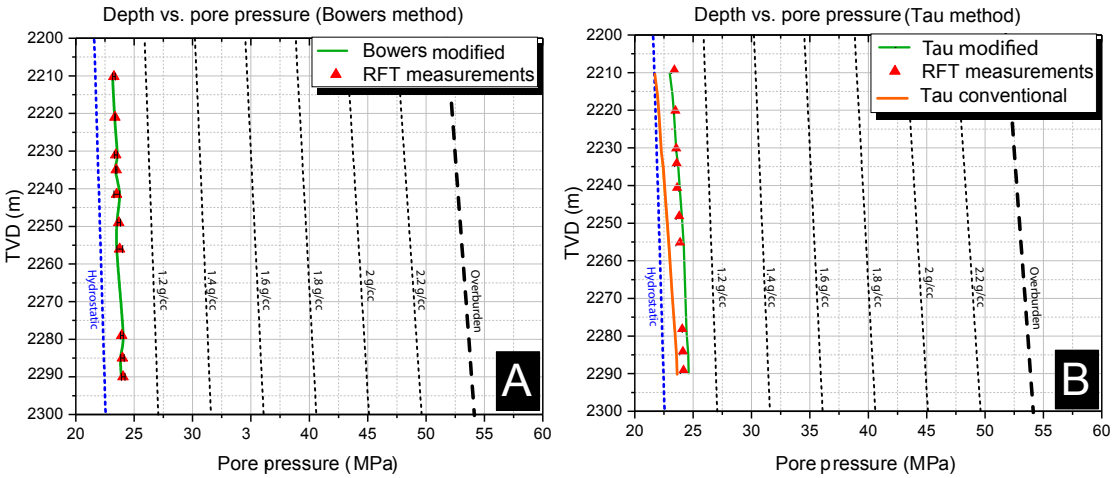

Figure 11: Pore pressure prediction based on Tau, and Bowers method along with the RFT measurements at a selected well location. (A) Modified Bowers produced relatively accurate predictions while extremely poor calibration of the Bowers made the estimation unreliable. (B) Comparing the conventional and modified Tau method show that the later improved the accuracy of the estimation.

four (mostly sandstone), while it failed to deliver the same results in cluster two (dolomite and limestone). These observations are in agreement with the principal assumption of the Bowers and Tau methods, indicating these techniques are most reliable in shale and sandstone (with a lower degree of certainty compared to shales), but they do not produce reliable results in carbonate settings. Overall, comparing the conventional methods with the proposed procedure shows significant improvement in pore pressure estimations. Table 3 summarized the quantitative comparison (MAPE and MSE) between conventional and proposed Tau methods.

We believe the most important sources of uncertainty in this research (and perhaps similar studies) is related to limited data in the formations above the reservoir, incorrect well logs values in some intervals within reservoir due to wellbore condition, noisy measurements, and lack of modern formation evaluation logs which can affect the clustering results (specially K-means) tremendously.

Method	MAPE %	MSE
Conventional Bowers	105	146
Bowers with proposed modifications	15.5	0.76
Conventional Tau	4	21761
Tau with proposed modifications	1	1840

Table 3: Comparing Tau methods with the results of the SOM improved estimations. Mean absolute percentage error and mean square error used as a measure of the accuracy of the predictions.

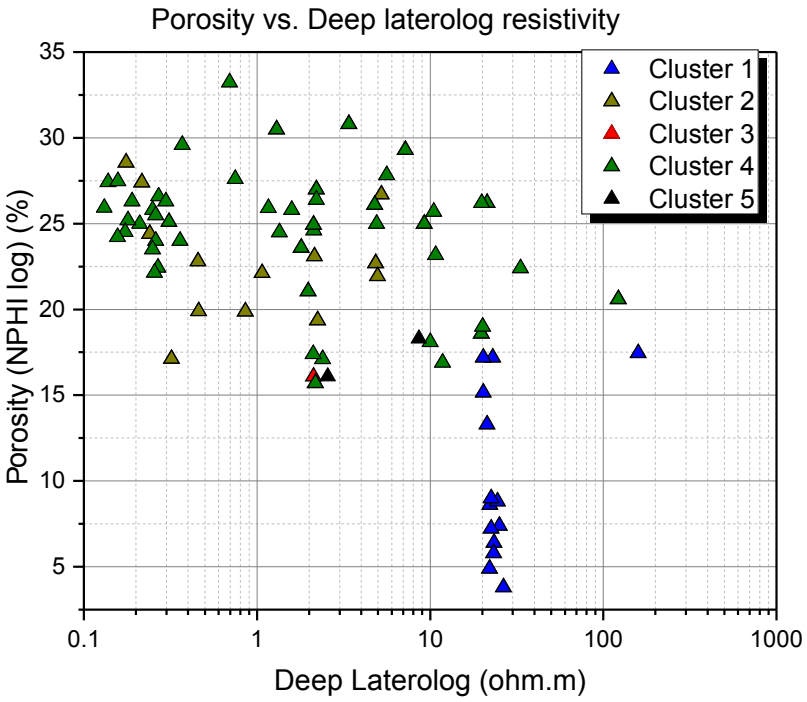

Figure 12: Cluster one shows notably low porosity and high resistivity compared to the other clusters. The porosity and resistivity characteristics of the cluster one could be an indicator of high amounts of silica minerals in the overall mineralogy of the unit.

4. Conclusions

Pore pressure perdition using velocity based methods (i.e., Eaton and Bowers methods) is not straightforward and require a clear understanding of the lithology and geomechanical state of the reservoir. Also, inaccurate calibration of the velocity versus effective stress, especially in a reservoir with complex lithology will introduce significant uncertainty in the final pressure estimation. In this research, we showed each major zones at offset test wells may have distinct compaction trends with different empirical constants. Also, the SOM algorithm is promising for lithofacies classification of well log data.

To carry out this study, we did not have access to more sophisticated lithology sensitive well logs such as Photoelectric Factor (PEF) and Pulsed Neutron Lifetime logs (PNL) as well Nuclear Magnetic Resonance (NMR); however, such information can be used to account for fluid content and saturation in the future studies. Overall, we conclude that in case of complex lithology the accuracy of the conventional Bowers and Tau methods can be improved by accurate calibration of the empirical equations for major lithostratigraphic units, leading to a reliable final pore pressure estimation.

Acknowledgments

The authors would like to thank S. Seyedali and A. Ahmadi for his major technical advice and many useful discussions. The authors are grateful to Iranian Offshore Oil Company (IOOC) for permission to use the seismic data and well logs.

Appendix - clustering methods

1. In the M-BSAS method, the mean vector for clusters will be updated as:

$$m_{C_k}^{new} = \frac{(n_{C_k}^{new} - 1)m_{C_k}^{old} + x}{m_{C_k}^{new}} \quad .1$$

where x is the value of the new data, C_k is cluster center, and $n_{C_k}^{new}$ is the cardinality of C_k after x assignment.

2. To introduce new centres for clusters after allocating a new data point to them in the K-means method, we can write:

$$S_i^{(t)} = \left\{ x_p : \|x_p - m_i^{(t)}\|^2 \leq \|x_p - m_j^{(t)}\|^2 \quad \forall j, 1 \leq j \leq k \right\} \quad .2$$

where x_p is the value of the new data, $m_i^{(t)}$ and $m_j^{(t)}$ are the center of the clusters and defined as:

$$m_i^{t+1} = \frac{1}{|S_i^t|} \sum_{x_j S_i^{(t)}} x_j \quad .3$$

where S_i is the number of data.

3.Mathematical definition of distance in Single linkage and complete linkage hierarchical methods can be written as:

$$d_{single}(G, H) = \min d_{ij}, i \in G, j \in H \quad .4$$

$$d_{complete}(G, H) = \max d_{ij}, i \in G, j \in H \quad .5$$

where $d_{i,j}$ is the distance between elements $i \in G$ and $j \in Y$, and G and H are two sets of elements (i.e., clusters).

References

Abu Abbas, O., 2008. Comparisons between data clustering algorithms. The International Arab Journal of Information Technology 5 (3), 320–325.

Ahmadi, M. A., Zendehboudi, S., Lohi, A., Elkamel, A., Chatzis, I., 2012. Reservoir permeability prediction by neural networks combined with hybrid genetic algorithm and particle swarm optimization. Vol. 61. pp. 582–598.

Ahmadi, N., Berangi, R., 2008. Modulation classification of qam and psk from their constellation using genetic algorithm and hierarchical clustering. In: Information and Communication Technologies: From Theory to Applications, 2008. ICTTA 2008. 3rd International Conference on. IEEE, pp. 1–5.

Aminzadeh, F., De Groot, P., 2006. Neural networks and other soft computing techniques with applications in the oil industry. Eage Publications.

Bohling, G., Dubois, M., 2003. An integrated application of neural network and markov chain techniques to prediction of lithofacies from well logs. Kansas Geol Survey Open File Report 50 (6).

Boitnott, G., Miller, T., Shafer, J., 2009. Pore pressure effects and permeability: effective stress issues for high pressure reservoirs. In: Proceedings of the International Symposium of the Society of Core Analysts (SCA'09). p. 9.

Bowers, G., 6 1995. Pore pressure estimation from velocity data: Accounting for overpressure mechanisms besides undercompaction. SPE Drilling and Completion 10 (2).

Bowers, G. L., et al., 1995. Pore pressure estimation from velocity data: Accounting for overpressure mechanisms besides undercompaction. SPE Drilling & Completion 10 (02), 89–95.

Carlsson, G., Mémoli, F., Ribeiro, A., Segarra, S., 2017. Admissible hierarchical clustering methods and algorithms for asymmetric networks. IEEE Transactions on Signal and Information Processing over Networks 3 (4), 711–727.

Chopra, S., Huffman, A. R., 2006. Velocity determination for pore-pressure prediction. The Leading Edge 25 (12), 1502–1515.

Ciampi, A., Lechevallier, Y., 2000. Clustering large, multi-level data sets: an approach based on kohonen self organizing maps. In: European Conference on Principles of Data Mining and Knowledge Discovery. Springer, pp. 353–358.

Coléou, T., Poupon, M., Azbel, K., 2003. Unsupervised seismic facies classification: A review and comparison of techniques and implementation. The Leading Edge 22 (10), 942–953.

Cranganu, C., 2013. Natural Gas and Petroleum: Production Strategies, Environmental Implications, and Future Challenges. Nova Publishers.

Cranganu, C., Soleymani, H., 2015. Carbon dioxide sealing capacity: Textural or compositional controls? a case study from the oklahoma panhandle. AAPG/DEG Environmental Geosciences 22 (2), 57–74.

Cranganu, C., Soleymani, H., Azad, S., Watson, K., 2014. Carbon dioxide sealing capacity: Textural or compositional controls? AAPG Search and Discovery Article# 41474.

Dell'Aversana, P., Ciurlo, B., Colombo, S., 2018. Integrated geophysics and machine learning for risk mitigation in exploration geosciences. In: 80th EAGE Conference and Exhibition 2018.

Di Giuseppe, M. G., Troiano, A., Troise, C., De Natale, G., 2014. k-means clustering as tool for multivariate geophysical data analysis. an application to shallow fault zone imaging. Journal of Applied Geophysics 101, 108–115.

Eaton, B. A., et al., 1972. The effect of overburden stress on geopressure prediction from well logs. Journal of Petroleum Technology 24 (08), 929–934.

Ehrenberg, S., Nadeau, P., Aqrawi, A., 2007. A comparison of khuff and arab reservoir potential throughout the middle east. AAPG bulletin 91 (3), 275–286.

Fouedjio, F., 2016. A hierarchical clustering method for multivariate geostatistical data. Spatial Statistics 18, 333–351.

Giles, M., Indrelid, S., James, D., 1998. Compactionthe great unknown in basin modelling. Geological Society, London, Special Publications 141 (1), 15–43.

Guglielmi, Y., Cappa, F., Avouac, J.-P., Henry, P., Elsworth, D., 2015. Seismicity triggered by fluid injection–induced aseismic slip. Science 348 (6240), 1224–1226.

Hao, F., Zhu, W., Zou, H., Li, P., 2015. Factors controlling petroleum accumulation and leakage in overpressured reservoirs. AAPG Bulletin 99 (5), 831–858.

Holm, G., 1998. How abnormal pressures affect hydrocarbon exploration, exploitation. Oil and Gas Journal 96, 79–84.

Hong, S., Kumar, D. P., Reddy, D. A., Choi, J., Kim, T. K., 2017. Excellent photocatalytic hydrogen production over cds nanorods via using noble metal-free copper molybdenum sulfide (cu2mos4) nanosheets as co-catalysts. Applied Surface Science 396, 421–429.

Hottmann, C., Johnson, R., et al., 1965. Estimation of formation pressures from log-derived shale properties. Journal of Petroleum Technology 17 (06), 717–722.

J.Doyle, L., H.Roberts, H., 1988. Carbonate-clastic transitions. Vol. 42. p. 304.

Jin, J., 1994. Bsas: a basic program for two-dimensional subsidence analysis in sedimentary basins. Computers & Geosciences 20 (9), 1329–1345.

Jouini, M. S., Keskes, N., 2017. Numerical estimation of rock properties and textural facies classification of core samples using x-ray computed tomography images. Applied Mathematical Modelling 41, 562–581.

Kainulainen, J., Kainulainen, J. J., 2002. Clustering algorithms: basics and visualization. Helsinki University of Technology, Laboratory of Computer and Information Science.

Kangazian, A., Pasandideh, M., 2016. Sedimentary environment and sequence stratigraphy of the asmari formation at khaviz anticline, zagros mountains, southwest iran. Open Journal of Geology 6 (02), 87.

Kohonen, T., 1998. The self-organizing map. Neurocomputing 21 (1-3), 1–6.

Kohonen, T., Honkela, T., 2007. Kohonen network. Scholarpedia 2 (1), 1568.

Kohonen, T., Somervuo, P., 2002. How to make large self-organizing maps for nonvectorial data. Neural networks 15 (8-9), 945–952.

Kourki, M., Riahi, M. A., 2014. Seismic facies analysis from pre-stack data using self-organizing maps. Journal of Geophysics and Engineering 11 (6), 065005.

Liu, L., Shen, G., Wang, Z., Yang, H., Han, H., Cheng, Y., 2018. Abnormal formation velocities and applications to pore pressure prediction. Journal of Applied Geophysics.

Mannon, T., Young, R., 2017. Pre-drill pore pressure modelling and post-well analysis using seismic interval velocity and seismic frequency-based methodologies: A deepwater well case study from mississippi canyon, gulf of mexico. Marine and Petroleum Geology 79, 176–187.

Moghimidarzi, S., Furth, P. G., Cesme, B., 2016. Predictive–tentative transit signal priority with self-organizing traffic signal control. Transportation Research Record: Journal of the Transportation Research Board (2557), 77–85.

Nelson, P. H., 2010. Sonic velocity and other petrophysical properties of source rocks of cody, mowry, shell creek, and thermopolis shales, bighorn basin, wyoming. Petroleum Systems and Geologic Assessment of Oil and Gas in the Bighorn Basin Province, Wyoming and Montana, US Geol. Surv. Digital Data Ser., DDS-69-D.

Nguyen, S. T., Hoang, S. K., Khuc, G. H., Tran, H. N., et al., 2015. Pore pressure and fracture gradient prediction for the challenging high pressure and high temperature well, hai thach field, block 05-2, nam con son basin, offshore vietnam: A case study. In: SPE/IATMI Asia Pacific Oil & Gas Conference and Exhibition. Society of Petroleum Engineers.

Nour, A., AlBinHassan, N., 2013. Seismic attributes and advanced computer algorithm method to predict formation pore pressure: Paleozoic sediments of northwest saudi arabia. In: IPTC 2013: International Petroleum Technology Conference.

Obradors-Prats, J., Rouainia, M., Aplin, A. C., Crook, A. J., 2016. Stress and pore pressure histories in complex tectonic settings predicted with coupled geomechanical-fluid flow models. Marine and Petroleum Geology 76, 464–477.

Oloruntobi, O., Adedigba, S., Khan, F., Chunduru, R., Butt, S., 2018. Overpressure prediction using the hydro-rotary specific energy concept. Journal of Natural Gas Science and Engineering 55, 243–253.

Oughton, R. H., Wooff, D. A., Hobbs, R. W., O'Connor, S. A., Swarbrick, R. E., 2015. Quantifying uncertainty in pore pressure estimation using bayesian networks, with application to use of an offset well. In: Petroleum Geostatistics 2015.

Oyana, T. J., Achenie, L. E., Heo, J., 2012. The new and computationally efficient mil-som algorithm: potential benefits for visualization and analysis of a large-scale high-dimensional clinically acquired geographic data. Computational and mathematical methods in medicine 2012.

Reddy, D., Jana, P. K., et al., 2012. Initialization for k-means clustering using voronoi diagram. Procedia Technology 4, 395–400.

Riahi, M., Soleymani, H., 2011. Velocity based pore pressure prediction-a case study at one of the iranian south west oil fields. In: 73rd EAGE Conference and Exhibition incorporating SPE EUROPEC 2011.

Saberhosseini, S. E., Ahangari, K., Alidoust, S., 2013. Stability analysis of a horizontal oil well in a strike-slip fault regime. Austrian J. Earth Sci 106 (2), 30–36.

Saraswat, P., Sen, M. K., 2012. Artificial immune-based self-organizing maps for seismic-facies analysis. Geophysics 77 (4), O45–O53.

Sarparandeh, M., Hezarkhani, A., 2016. Application of self-organizing map for exploration of rees deposition. Open Journal of Geology 6 (07), 571.

Sfidari, E., Kadkhodaie-Ilkhchi, A., Rahimpour-Bbonab, H., Soltani, B., 2014. A hybrid approach for litho-facies characterization in the framework of sequence stratigraphy: a case study from the south pars gas field, the persian gulf basin. Journal of Petroleum Science and Engineering 121, 87–102.

Shahreza, M. L., Moazzami, D., Moshiri, B., Delavar, M., 2011. Anomaly detection using a self-organizing map and particle swarm optimization. Scientia Iranica 18 (6), 1460–1468.

Sheng, Y.-N., Guan, Z.-C., Xu, Y.-Q., 2017. Quantitative description method for uncertainty of formation pore pressure. Arabian Journal for Science and Engineering, 1–9.

Soleymani, H., Riahi, M.-A., 2012. Velocity based pore pressure predictiona case study at one of the iranian southwest oil fields. Journal of Petroleum Science and Engineering 94, 40–46.

Tasdemir, K., Merényi, E., 2009. Exploiting data topology in visualization and clustering of self-organizing maps. IEEE Transactions on Neural Networks 20 (4), 549–562.

Terzaghi, K., 1925. Principles of soil mechanics, ivsettlement and consolidation of clay. Engineering News-Record 95 (3), 874–878.

Theodoridis, S., Pikrakis, A., Koutroumbas, K., Cavouras, D., 2010. Introduction to pattern recognition: a matlab approach. Academic Press.

Tucker, M. E., 2003. Mixed clasticcarbonate cycles and sequences: Quaternary of egypt and carboniferous of england. Vol. 56. pp. 19–37.

Ugwu, G., 2015. Pore pressure prediction using offset well logs: Insight from onshore niger delta, nigeria. American Journal of Geophysics, Geochemistry and Geosystems 1 (3), 77–86.

Van Buchem, F., Allan, T., Laursen, G., Lotfpour, M., Moallemi, A., Monibi, S., Motiei, H., Pickard, N., Tahmasbi, A., Vedrenne, V., et al., 2010. Regional stratigraphic architecture and reservoir types of the oligo-miocene deposits in the dezful embayment (asmari and pabdeh formations) sw iran. Geological Society, London, Special Publications 329 (1), 219–263.

Wang, Z., Wang, R., 2015. Pore pressure prediction using geophysical methods in carbonate reservoirs: Current status, challenges and way ahead. Journal of Natural Gas Science and Engineering 27, 986–993.

Wild, K., Amann, F., Martin, C., et al., 2015. Some fundamental hydro-mechanical processes relevant for understanding the pore pressure response around excavations in low permeable clay rocks. In: 13th ISRM International Congress of Rock Mechanics. International Society for Rock Mechanics.

Wohlberg, B., Tartakovsky, D. M., Guadagnini, A., 2006. Subsurface characterization with support vector machines. IEEE Transactions on Geoscience and Remote Sensing 44 (1), 47–57.

Yang, F.-M., Huang, K.-Y., et al., 1991. Multilayer perceptron for detection of seismic anomalies. In: 1991 SEG Annual Meeting. Society of Exploration Geophysicists.

Zhang, J., 2011. Pore pressure prediction from well logs: Methods, modifications, and new approaches. Earth-Science Reviews 108 (1-2), 50–63.

Zhao, S., Zhou, Y., Wang, M., Xin, X., Chen, F., 2014. Thickness, porosity, and permeability prediction: comparative studies and application of the geostatistical modeling in an oil field. Environmental Systems Research 3 (1), 7.